Behavior of Bare, Cr3C2-20NiCr, and NiCrAlY coated Fe-Ni Based Superalloy Under Hot Corrosion in a 75 wt.% Na2SO4 + 25wt.% NaCl film at 9000C

Selly Septianissa[1], Ayu Zahra Chandrasari[2]
[1,2] Department of Mechanical Engineering, Faculty of Engineering, Widyatama University,
Bandung 40125, Indonesia
Email: selly.septianissa@widyatama.ac.id

Abstract

The main aim of this research is to assess the resistance to hot corrosion of untreated Fe-Ni-based superalloys compared to those coated with Cr3C2-20NiCr and NiCrAlY. These superalloys are strengthened through precipitation with ɣ' Ni3(Al, Ti) and further fortified using high-velocity oxy-fuel (HVOF) thermal spray coating. The evaluation is performed under harsh conditions consisting at a temperature of 900°C for a duration of 25 cycles in a mixture containing 75 wt.% Na2SO4 and 25 wt.% NaCl. An optical microscope (OM) is utilized to determine the coating thickness of the coated specimens. Corrosion kinetics are evaluated by measuring changes in mass at the conclusion of each cycle during the investigation of hot corrosion. Furthermore, X-ray diffraction (XRD), energy dispersive spectroscopy (EDS), and scanning electron microscopy (SEM) are employed to investigate the chemical composition, ascertain phases, and scrutinize the surface morphology of the corrosion products. The findings reveal that the Fe-Ni superalloy, coated with precipitation-strengthened layers, demonstrates enhanced resistance to hot corrosion compared to the uncoated substrates, as evidenced by reduced weight gain per unit area. The coated substrates are enveloped by protective oxide layers consisting of chromium, nickel, aluminum, and their respective spinels, effectively shielding the substrate surfaces. In contrast, The superalloy without coating, which underwent precipitation hardening within the substrate, showed instances of microspalling and sputtering of the oxide scale. Findings suggested that both Cr3C2-20NiCr and NiCrAlY coatings substantially improved resistance against hot corrosion. Noteworthy was the superior protective efficacy of the NiCrAlY coating over the Cr3C2-20NiCr layer, attributed to the development of protective oxide scales containing Cr2O3 and NiCr2O4.

Keywords: *Superalloy, thermal spray coating, HVOF, NiCrAlY; Cr3C2-20 NiCr, hot corrosion.*

– – – – – – – – – – ◆ – – – – – – – – – –

A. INTRODUCTION

Because of its high temperature characteristics, superalloy is frequently used in gas turbines, petrochemical plants, power plants, cars, airplanes, and waste heat incinerators [1-3]. The A286 superalloy is identified as a precipitation-hardenable austenitic stainless steel recognized for its structured face-centered cubic (FCC) gamma prime (γ′) Ni3(Al, Ti) phase [4-7]. It is renowned for its outstanding mechanical strength at elevated temperatures and resistance to corrosion, this alloy demonstrates remarkable efficacy in acidic surroundings, notably those laden with sulfuric acid, chlorine, and hydrogen, especially under favorable conditions [8-9].

Hot corrosion of metals and their alloys poses a significant challenge in high-temperature environments where coal and biomass serve as fuel sources. This problem is widespread in various applications including gas turbines, boilers, superheaters in power plants, and facilities for incinerating waste heat [1-3]. The primary mechanisms leading to high-temperature hot corrosion involve degradation processes occurring both with and without the presence of a molten salt environment. In the coal-fired boiler, the hot corrosion issue that has been impacting the thermal. Various corrosive products such as Natrium, Chroline, Sulphur, and Vanadium are the primary offenders that cause the turbine to corrode and produce a highly corrosive product [4-6]. Na2SO4, V2O5, K2SO4, KCl and NaCl are the corrosive products undergo oxidation and high-temperature reactions with one another. [7].

As such, superalloys need a covering that can withstand corrosion at high temperatures for use in gas turbines, boilers, ships, and airplanes [10,11]. In contemporary times, thermal spray coating methods including arc spray coating, flame plasma spray coating, high-velocity oxy-fuel (HVOF), detonation gun, and cold spray coating are utilized to safeguard superalloy materials against high-temperature oxidation and corrosion [3, 9]. Among these, the HVOF coating is distinguished by its compactness, low porosity, strong bonding, enhanced hardness, and superior resistance to wear and corrosion, providing it with significant performance advantages over other thermal spray coating methods [3, 9, 12]. In applications necessitating protection against oxidation and hot corrosion, coatings such as Ni-20%Cr, Cr3C2-25%NiCr, NiCrAlY, Ni3Al, and stellite are employed. [12-16]. Numerous investigations have highlighted the utility of Cr3C2-NiCr coatings in withstanding high-temperature wear and corrosion within gas turbine and boiler settings. The corrosion resistance is primarily attributed to NiCr, while Cr3C2 serves to alleviate the stress induced during thermal cycling in real boiler operating conditions [3, 17]. NiCrAlY coatings offer protection against both hot corrosion and high-temperature oxidation by virtue of their capacity to develop a compact and firmly adherent Al2O3 scale on the surface of the coating [18, 19].

Septianissa et al. (2022) assessed the hot corrosion performance of Fe-Ni superalloy with and without coating at 900°C, albeit their study only presented thermogravimetric analysis for 13 cycles. In this study, the cyclic hot corrosion resistance of the Fe-Ni superalloy without coating, and the same superalloy coated with Cr3C2-20NiCr and NiCrAlY, was investigated in a corrosive environment containing 75 wt.% Na2SO4 + 25 wt.% NaCl at 900°C for 25 cycles. The corrosion kinetics of both uncoated and HVOF-coated specimens subjected to hot corrosion were assessed through thermogravimetric tests.

B. METHOD

Table 1 display the Fe-Ni Superalloy nominal chemical composition of the substrate material is utilized to generate the required formulation γ'-Ni3Al, this alloy is created in a laboratory using a Direct Current Electric Arc Furnace (DC-EAF) for 45 minutes. In order to homogenize the alloy component under the protection of the inert

gas argon on horizontal furnaces. the speciments were first homogenized at 1150oC for 5 hours. Then, the specimens were subjected to solid solution heat treatment 980oC for 1h subsequently water quenched and isothermally aged at 840oC for 4h to get the appropriate microstructure.

Table 1. The Fe-Ni superalloy's chemical composition (weight percentage)

Alloy	Fe	Ni	Al	Cr	Ti	Mo
Fe-Ni alloy	balance	26	0.8	15	2	0.25

For coating, specimens with dimension 15 x 15 x 3 mm were cut using a wire cutter. The specimens were prepared by grit blasting with alumina paste after being polished with 60, 100, 120, 1000, 1200, 1500, 2000, and 5000 grid SiC sheets. Acetone was then used to clean the specimens to remove the oxide. After that, the substrate's oxide layer and contaminants were removed the superalloy material was coated with NiCrAlY and Cr3C2-20%NiCr powder using the HVOF process, employing distilled water and acetone. Table 2 reports the process parameters used for the thermal spray coating.

Table 2. An element of the high velocity oxy-fuel procedure

Parameters	Values
Oxygen Pressure	8 bar
Oxygen flow rate	270 liter/min
Propane pressure	5,5 bar
Propane flow rate	62,4 liter/min
Nitrogen pressure	5 bar
Nitrogen flow rate	8 liter/min
Air pressure	6,2 bar
Spay distance	250 mm

Using molten salt made up of 75wt.% Na2SO4 and 25wt.% NaCl, 25 cycles of cyclic hot corrosion were applied to the Fe-Ni superalloy without coating, the NiCrAlY-coated layers, and the superalloy coated with Cr3C2-20%NiCr. Every cycle included a one-hour heating period in the muffle furnace at 900 oC and a twenty-minute cooling period at room temperature. Using a brush, a layer of 75wt.% Na2SO4 and 25wt.% NaCl Salt was administered onto the heated polished sample at a rate of 3-5 mg/cm2. To remove moisture content, the specimens coated with salt were dried for two hours at 110oC. After drying, the specimens weight were measured when each cycle concludes, in addition to the spalled. After concluding the hot corrosion experiment, SEM/EDS analysis (SU3500, Hitachi High-Tech America) was aimed To

examine the composition, surface morphology, and cross-sectional attributes of the corrosion products, an analysis was conducted. Additionally, XRD analysis was employed to identify the phases present, utilizing the RIGAKU Smartlab 3Kw 2080B212 model instrument. The outcomes aligned with the anticipated phase identification.

C. RESULTS AND DISCUSSION

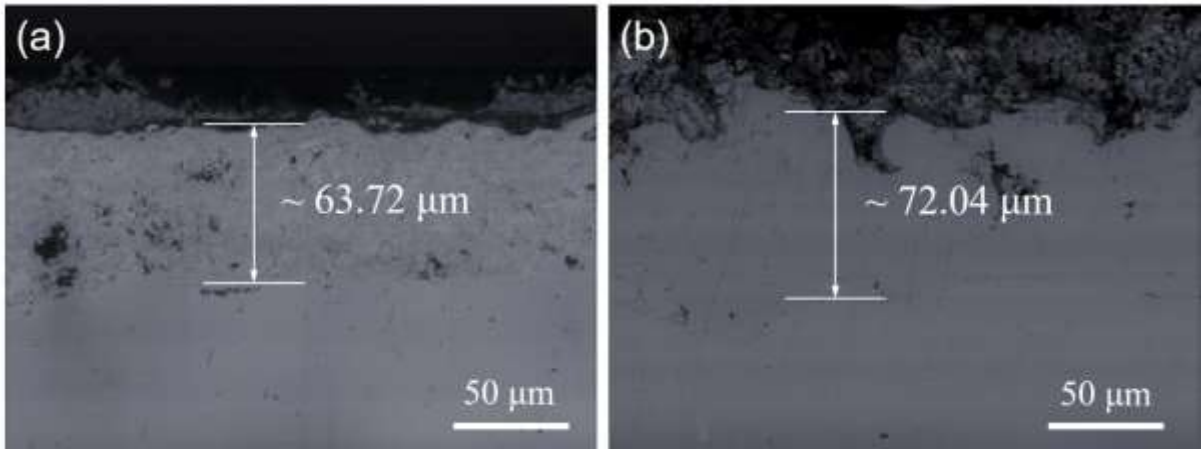

Fig. 1. Cr3C2-NiCr and NiCrAlY coated with the optical microstructure observed in cross-section of the Fe-Ni superalloy fabricated via HVOF thermal spray spraying.

The cross-sectional optical imaging micrographs of the Cr3C2-NiCr and NiCrAlY coatings in their as-sprayed state are depicted in Figures 1(a) and (b) respectively. The HVOF thermal spray coating technique demonstrated its efficacy in applying these coatings onto the Fe-Ni superalloy. Measurements revealed that the Cr3C2-NiCr and NiCrAlY coatings had The thicknesses measured approximately 63.72 µm and 72.04 µm, respectively. Notably, microscopic pores were visible in the Cr3C2-NiCr coated specimen as depicted in Figure 1(a).

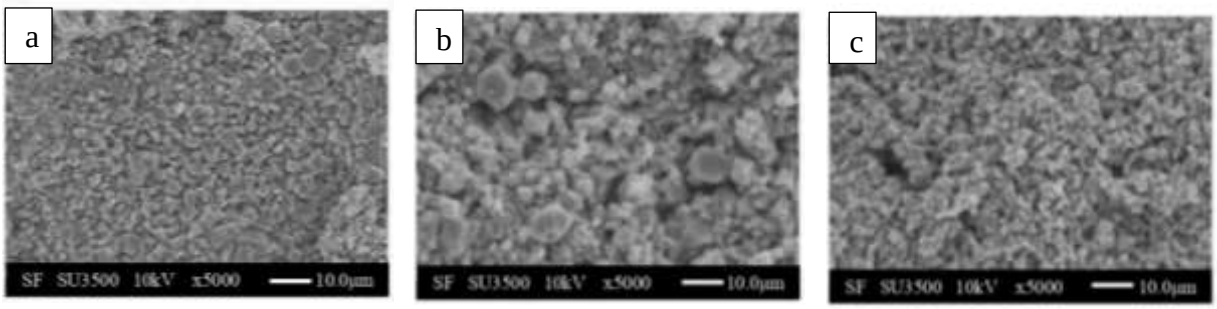

Fig. 2. The oxide scale surface morphologies that developed on the specimen when it was contacted with the melted salt for 25 cycles of (a) coated Cr3C2-NiCr, (b) coated NiCrAlY, and (c) uncoated Fe-Ni superalloy

Figure 2 illustrates the SEM surface microstructure of both the untreated The Fe-Ni superalloy and the Fe-Ni superalloy with coatings of Cr3C2-20%NiCr and NiCrAlY, as well as NiCrAlY applied via HVOF thermal spray spraying, after exposure to the experiment was conducted in a molten salt environment consisting of

75 wt.% Na2SO4 + 25 wt.% NaCl for 25 cycles at 900°C. The results suggest that an escalation in the number of cycles during hot corrosion testing results in a more pronounced surface morphology structure. Additionally, the substrate may be effectively coated with partially and totally melted Cr3C2-20%NiCr and NiCrAlY particles coated with Fe-Ni superalloy (Fig. 2(a) and (b)). Additional analysis of the surface morphologies of the microscopic granular structures of the uncoated superalloy (Fig. 2(c)) and the hot-corroded coated Cr3C2-20%NiCr Fe-Ni superalloy (Fig. 2(a)). Conversely, the surface morphologies depicted in Figure 2(b), the depiction of the angular structure of the NiCrAlY layer applied to the Fe-Ni superalloy suggests that Al2O3 can function as a protective oxide layer, thus offering an advantage in the pursuit of improved corrosion resistance.

Fig. 3. The XRD patern for (a) the uncoated Fe-Ni superalloy, (b) the NiCrAlY-coated substrate, (c) the Cr3C2-20%NiCr-coated substrate post hot corrosion exposure

The X-ray diffraction (XRD) profiles of uncoated and coated Fe-Ni superalloys, following HVOF thermal spraying and subsequent exposure to a hot corrosion regimen in the X-ray diffraction (XRD) patterns obtained from subjecting both uncoated and coated Fe-Ni superalloys to a hot corrosion test in molten salt (75 wt.% Na2SO4 + 25 wt.% NaCl) for 50 cycles at 900°C are illustrated in Figures 5(a) through (c). A thorough examination of XRD data for all substrate materials, encompassing both coated and uncoated specimens, is available in our antecedent publication [20]. The predominant phases identified in The uncoated Fe-Ni superalloy showed the existence of Fe2O3, Al2O3, FeS, and NiCr2O4 in its composition. Analysis of the oxide scale revealed predominant peaks corresponding of NiCr2O4, Cr2O3, Fe2O3, and Al2O3 as major peaks, along with minor peaks corresponding to NiFe2O4 and NiO (see Fig. 3(a)). Conversely, in the case of the Cr3C2-20%NiCr coated specimen, primary phases identified included spinel NiCr2O4, Cr2O3, Fe2O3, and Al2O3, accompanied by minor phases such as NiO, NiFe2O4, FeS, and NiS (see Fig. 3(c)). Additionally, analysis of the XRD pattern for NiCrAlY coated substrates unveiled predominant phases comprising Aluminum oxide (Al2O3), chromium oxide (Cr2O3), iron oxide (Fe2O3), and spinel nickel chromate (NiCr2O4) were identified as major peaks, while minor peaks attributed to nickel oxide (NiO) and iron sulfide (FeS) were observed (refer to Fig. 3(b)).

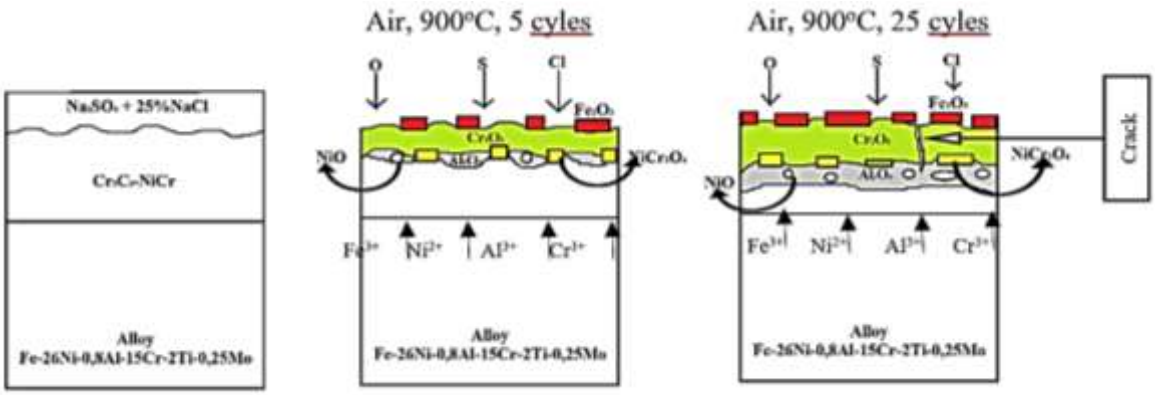

Fig. 5. Schematic representations of the Cr3C2-20%NiCr coating's hot corrosion processes

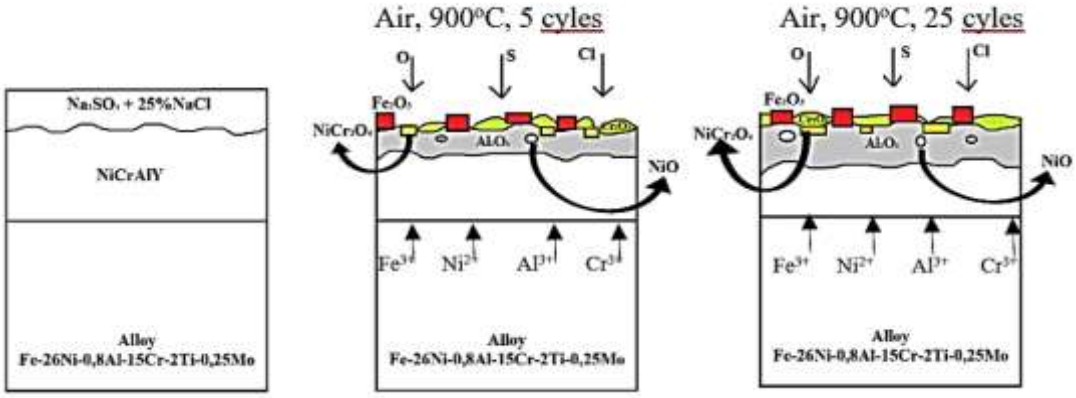

Fig. 6. Schematic representations of the NiCrAlY coating's hOT corrosion processes

Reduced weight gain is a clear indication that further ternary oxide production, such as NiCr2O4, is enhancing the oxidation resistance in molten salt media for coated, uncoated, and Cr3C2-20%NiCr Fe-Ni superalloys. At 900°C under hot corrosion conditions, the Cr3C2-20%NiCr and NiCrAlY coatings, after being subjected to corrosion, exhibit a minor surface phase identified as Fe2O3, which facilitates the diffusion of iron (Fe) from the substrate [21]. According to as per the XRD findings, both coated and uncoated superalloys show the presence of metal sulfides like FeS, CrS, and NiS. The implies that the components of the molten salt have penetrated the splat boundaries and could split at the oxide scale-substrate contact, thereby accelerating the oxidation process [12, 22]. The following equation explains this [25].

$$Na2SO4 \rightarrow Na2O + SO3$$

At 400°C, chlorine demonstrates the capacity to dissolve oxide scales and augment the formation of cracks within them. Subsequently, oxygen (O) and chlorine (Cl) interact with substrate elements involved in alloying such as chromium (Cr), nickel (Ni), and iron (Fe), facilitating the generation of volatile metal chlorides like Cr3Cl2, NiCl2, and FeCl2 through the fissures [22, 23]. On oxide scales, the production of volatile chloride may cause fractures. Afterwards, Cracks may arise from heat cycles brought on by different The thermal expansion rates differ between the oxide scale and the substrate material [24]. The following equation explains how sodium chloride (NaCl) combines with oxides to generate sodium chromate, which in turn releases volatile chlorine [26-27].

$$8NaCl\ (l) + 2Cr2O3\ (s) + 5O2\ (g) \rightarrow 4Na2CrO4\ (s) + 4Cl2\ (g)$$

By preventing reactive species from diffusing into the substrate alloys, Al2O3 and Cr2O3 might be able to aid moderately slow down the substrate material's oxidation . However, they increase corrosion resistance by preventing corrosion products from interacting with coating alloying elements. [28].

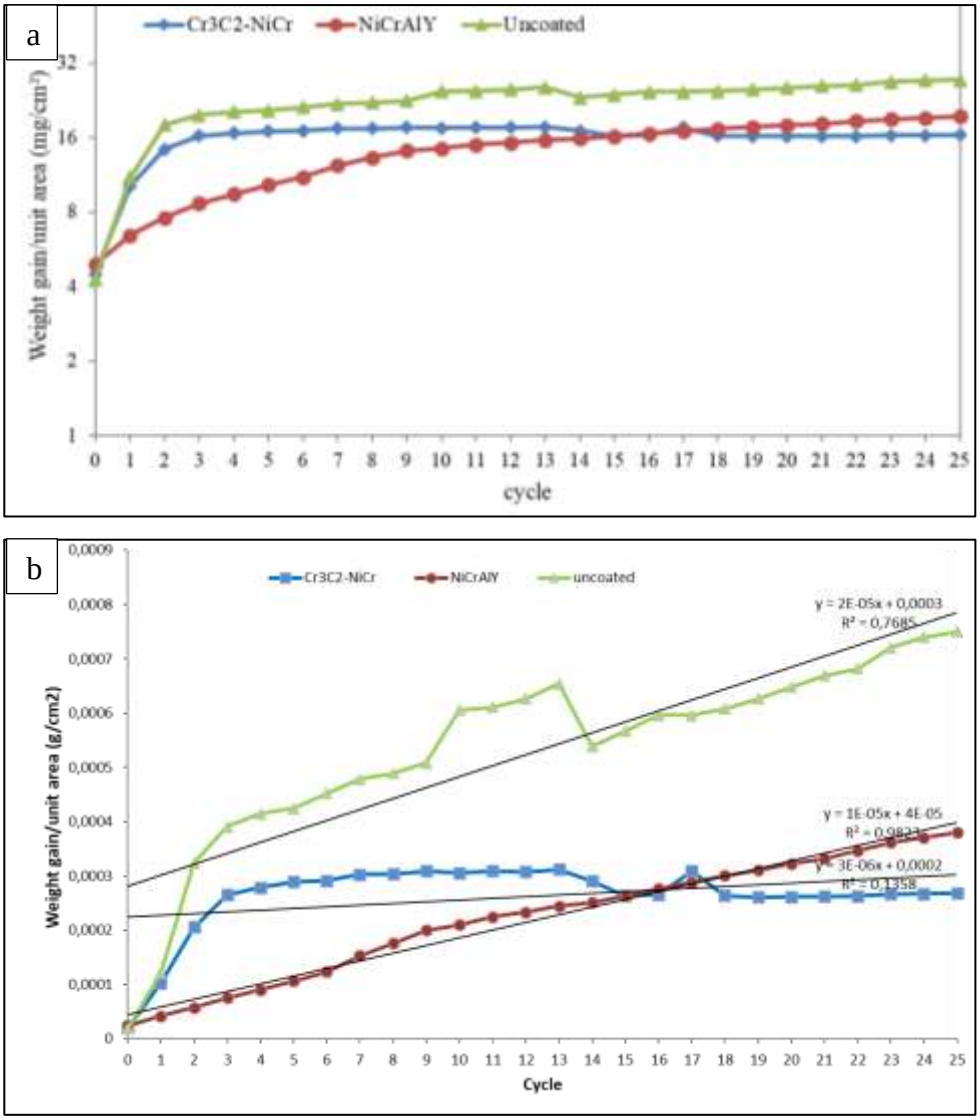

Fig. 6. (a) The graphs display the relationship between weight gain per unit area and cycle count. Additionally, graph (b) illustrates the relationship between the square of weight per unit area and cycle count specifically for the Cr3C2-NiCr coating, NiCrAlY superalloy covered with 75 wt.% Na2SO4 + 25wt.% NaCl molten salt following hot corrosion test with 25 cycles.

Figure 6 depicts the cumulative mass gain plots for The Fe-Ni superalloy without coating, the Fe-Ni superalloy with a coating of Cr3C2-NiCr, along with the thermal spray layers of NiCrAlY were investigated concerning their response to exposure to the Fe-Ni superalloy underwent exposure to molten salt, consisting of 75 wt.% Na2SO4 + 25 wt.% NaCl, for 50 cycles. It was observed that during the first fifteen cycles, the weight gain of the Cr3C2-20% NiCr layer and the uncoated Fe-Ni superalloy surpassed that of the Fe-Ni superalloy coated with NiCrAlY, attributable to the effects of the hot corrosion process. This highlights the substantial enhancement in corrosion resistance achieved through the presence of coatings applied via HVOF thermal spray spraying on the Fe-Ni superalloy. Comparative analysis revealed that the NiCrAlY coating material offers NiCrAlY layer demonstrates superior corrosion

resistance when contrasted with the Cr3C2-NiCr layer. Nevertheless, beyond the 15th cycle of the NiCrAlY coating, a gradual increase in weight was observed, and it was noted that the coated superalloys consistently exhibited significantly less weight growth as coated superalloy demonstrates a greater resistance to corrosion than the uncoated counterpart when exposed to the specified molten salt environment. As a result, minimal alterations in weight were linked to the sputtering of the oxide scale. Table 3 presents the cumulative weight growth and the parabolic constant Kp (expressed in 10^-5g^2cm^-4s^-1). The relationship between (ΔW/A)^2 and the number of cycles, the equation, depicted in the form of (ΔW/A)^2 = Kp t, where t denotes the number of cycles and ΔW/A represents the weight per unit area (g/cm^2), illustrates the derivation of the parabolic constant Kp using a linear least-squares technique (refer to Fig. 4(b)).

Table 3. Parabolic rate constant (Kp)

Sampel	Kp ($10^{-5}g^2cm^{-4}s^{-1}$)
Cr_3C_2-NiCr *coated*	7.09
NiCrAlY *coated*	4.9
Uncoated	4.3

The parabolic constants have been established for the untreated Fe-Ni superalloy, the Fe-Ni superalloy coated with Cr3C2-20%NiCr, and the NiCrAlY-coated superalloy -coated superalloy to be 4.3 x 10^-5, 7.09 x 10^-5, and 4.9 x 10^-5 g^2cm^-4s^-1, respectively, as determined from the hot corrosion examinations, the cumulative weight gains for the Cr3C2-20%NiCr-coated superalloy, the NiCrAlY-coated superalloy, and the observed weight gains for the uncoated Fe-Ni superalloy are documented as 27.3854, 16.3651, and 19.4927 mg/cm^2, respectively. A comparative examination, as illustrated in Figure 4, indicates that both the Cr3C2-20%NiCr and NiCrAlY coatings exhibit a reduction in weight gain compared to the absence of coating on the Fe-Ni superalloy coatings effectively decrease the overall weight increase The Cr3C2-20%NiCr film performs best for hot corrosion resistance after the 15th cycle, as the least amount of weight gain suggests.

D. CONCLUSION

The successful application of NiCrAlY and Cr3C2-20%NiCr coatings applied to a superalloy based on ferro nickel (Fe-Ni) substrates has been accomplished by leveraging knowledge obtained from the HVOF thermal spray coating process. These coatings, administered via HVOF, significantly improve corrosion resistance in the superalloy, as evidenced by a decreased weight gain when compared to the uncoated substrate. The highest weight increases recorded the weight gains for the uncoated Fe-Ni superalloy, the Fe-Ni superalloy coated with Cr3C2-20%NiCr, and the NiCrAlY-coated superalloy are 27.3854, 16.3651, and 19.4927 mg/cm^2, respectively.

Additionally, the parabolic constants for these materials are determined to be 4.3 x 10^-5, 7.09 x 10^-5, and 4.9 x 10^-5 g^2cm^-4s^-1, respectively.

The production of thick, adherent, and stable Cr2O3 in Cr3C2-20%NiCr covered with Fe-Ni superalloy leads to superior corrosion resistance after the 15th cycle compared to the uncoated supperalloy and the supperalloy coated NiCrAlY based on the findings in the molten salt environment of NaCl. Conversely, studies have indicated that the untreated Fe-Ni superalloy exhibits sulfur as a corrosive agent, accelerating corrosion through the mechanism of sulphidation. Prior to the fifteenth cycle, chlorine, a corrosive component present in the application of the Cr3C2-20%NiCr HVOF thermal spray material onto the superalloy, was observed, experienced an escalation, thereby accelerating the corrosion attack rate through the chlorination process. This mechanism involves the diffusion of molten salt and the formation of oxide film-corrosive components resulting from segregates [20].

E. ACKNOWLEDGMENT

The Department of Metallurgical, Engineering of Mining and Petroleum Engineering, Institut Teknologi Bandung (ITB), and the Department of Mechanical Engineering, Engineering Faculty, Widyatama University, are sincerely acknowledged by the authors for their support. We express our gratitude to the specialists at the National Research and Innovation Agency's Research Center for Advanced Materials. We also value the cooperation and assistance provided by each and every research assistant at the ITB Metal Sustainability and Corrosion Laboratory. The National Research and Innovation Agency provided funding for this project.

REFERENCES

1. Chen, S., Zhao, M., & Rong, L. (2013). Effect of Ti content on the microstructure and mechanical properties of electron beam welds in Fe–Ni based alloys. Materials Science and Engineering: A, 571, 33-37.
2. Mustafa, A. H., Hashmi, M. S., Yilbas, B. S., & Sunar, M. (2008). Investigation into thermal stresses in gas turbine transition-piece: Influence of material properties on stress levels. Journal of Materials Processing Technology, 201(1-3), 369-373.
3. Muthu, S. M., Arivarasu, M., Krishna, T. H., Ganguly, S., Prabhakar, K. P., & Mohanty, S. (2020). Improvement in hot corrosion resistance of dissimilar alloy 825 and AISI 321 CO 2-laser weldment by HVOF coating in aggressive salt environment at 900 C. International Journal of Minerals, Metallurgy and Materials, 27, 1536-1550.
4. Mustafa, A. H., Hashmi, M. S., Yilbas, B. S., & Sunar, M. (2008). Investigation into thermal stresses in gas turbine transition-piece: Influence of material properties on stress levels. Journal of Materials Processing Technology, 201(1-3), 369-373.
5. Singhal, L. K., & Martin, J. W. (1968). The mechanism of tensile yield in an age-hardened steel containing γ′(ordered Ni3Ti) precipitates. Acta Metallurgica, 16(7), 947-953.

6. Thompson, A. W., & Brooks, J. A. (1982). The mechanism of precipitation strengthening in an iron-base superalloy. Acta Metallurgica, 30(12), 2197-2203.
7. Zhang, P., Zhu, Q., Hu, C., Wang, C. J., Chen, G., & Qin, H. Y. (2015). Cyclic deformation behavior of a nickel-base superalloy under fatigue loading. Materials & Design, 69, 12-21.
8. Martín, Ó., De Tiedra, P., & San-Juan, M. (2017). Combined effect of resistance spot welding and precipitation hardening on tensile shear load bearing capacity of A286 superalloy. Materials Science and Engineering: A, 688, 309-314.
9. Muthu, S. M., & Arivarasu, M. (2019). Oxidation and hot corrosion studies on Fe-based superalloy A-286 pulsed current GTA weldments in gas turbine environment. Materials Research Express, 6(11), 116577.
10. Sidhu, T. S., Agrawal, R. D., & Prakash, S. (2005). Hot corrosion of some superalloys and role of high-velocity oxy-fuel spray coatings—a review. Surface and coatings technology, 198(1-3), 441-446.
11. Singh, J., Vasudev, H., & Singh, S. (2020). Performance of different coating materials against high temperature oxidation in boiler tubes–A review. Materials Today: Proceedings, 26, 972-978.
12. Reddy, N. C., Koppad, P. G., Reddappa, H. N., Ramesh, M. R., Babu, E. R., & Varol, T. E. M. E. L. (2019). Hot corrosion behaviour of HVOF sprayed Ni3Ti and Ni3Ti+(Cr3C2+ 20NiCr) coatings in presence of Na2SO4-40% V2O5 at 650° C. Surface Topography: Metrology and Properties, 7(2), 025019.
13. Singh, H., Puri, D., & Prakash, S. (2007). An overview of Na 2 SO 4 and/or V 2 O 5 induced hot corrosion of Fe-and Ni-based superalloys. Rev. Adv. Mater. Sci, 16(1-2), 27-50.
14. Zhang, Y. J., Sun, X. F., Guan, H. R., & Hu, Z. Q. (2002). 1050 C isothermal oxidation behavior of detonation gun sprayed NiCrAlY coating. Surface and Coatings Technology, 161(2-3), 302-305.
15. Sidhu, B. S., & Prakash, S. (2006). Performance of NiCrAlY, Ni–Cr, Stellite-6 and Ni3Al coatings in Na2SO4–60% V2O5 environment at 900 C under cyclic conditions. Surface and Coatings Technology, 201(3-4), 1643-1654.
16. Sidhu, T. S., Prakash, S., & Agrawal, R. D. (2006). Evaluation of hot corrosion resistance of HVOF coatings on a Ni-based superalloy in molten salt environment. Materials science and engineering: A, 430(1-2), 64-78.
17. Goyal, K., & Goyal, R. (2020). Improving hot corrosion resistance of Cr3C2–20NiCr coatings with CNT reinforcements. Surface engineering, 36(11), 1200-1209.
18. Wang, J., Chen, M., Cheng, Y., Yang, L., Bao, Z., Liu, L., ... & Wang, F. (2017). Hot corrosion of arc ion plating NiCrAlY and sputtered nanocrystalline coatings on a nickel-based single-crystal superalloy. Corrosion Science, 123, 27-39.

19. Ren, X., & Wang, F. (2006). High-temperature oxidation and hot-corrosion behavior of a sputtered NiCrAlY coating with and without aluminizing. Surface and Coatings Technology, 201(1-2), 30-37.
20. Septianissa, S., Prawara, B., Basuki, E. A., Martides, E., & Riyanto, E. (2022). Improving the hot corrosion resistance of γ/γ'in Fe-Ni superalloy coated with Cr3C2-20NiCr and NiCrAlY using HVOF thermal spray coating. International Journal of Electrochemical Science, 17(12), 221231.
21. Wang, H., Yan, X., Zhang, H., Gee, M., Zhao, C., Liu, X., & Song, X. (2019). Oxidation-dominated wear behaviors of carbide-based cermets: A comparison between WC-WB-Co and Cr3C2-NiCr coatings. Ceramics International, 45(17), 21293-21307.
22. Kamal, S., Jayaganthan, R., Prakash, S., & Kumar, S. (2008). Hot corrosion behavior of detonation gun sprayed Cr3C2–NiCr coatings on Ni and Fe-based superalloys in Na2SO4–60% V2O5 environment at 900 C. Journal of alloys and compounds, 463(1-2), 358-372.
23. Papp, J., Hehemann, R. F., & Troiano, A. R. (1974). Hydrogen embrittlement of high strength fcc alloys. Hydrogen in metals, 1974.
24. Nithin, H. S., Nishchitha, K. M., Shamanth, V., Hemanth, K., & Babu, K. A. (2020). High-Temperature Oxidation and Corrosion Behaviour of APS CoCrAlY+ Cr 3 C 2–NiCr Composite Coating. Journal of Bio-and Tribo-Corrosion, 6(2), 28.
25. Guo, M. H., Wang, Q. M., Ke, P. L., Gong, J., Sun, C., Huang, R. F., & Wen, L. S. (2006). The preparation and hot corrosion resistance of gradient NiCoCrAlYSiB coatings. Surface and Coatings Technology, 200(12-13), 3942-3949.
26. McKee, D. W., Shores, D. A., & Luthra, K. L. (1978). The effect of SO 2 and NaCl on high temperature hot corrosion. Journal of the Electrochemical Society, 125(3), 411.
27. Chen, Lingyun, Hao Lan, Chuanbing Huang, Bin Yang, Lingzhong Du, and Weigang Zhang. "Hot corrosion behavior of porous nickel-based alloys containing molybdenum in the presence of NaCl at 750° C." Engineering Failure Analysis 79 (2017): 245-252.
28. Nicoll, A. R., & Wahl, G. (1982). The effect of alloying additions on MCrAlY systems—An experimental study. Thin Solid Films, 95(1), 21-34.